Steel and Composite Structures, *Vol. 16, No. 4* (*2014*) *339-356*
DOI: http://dx.doi.org/10.12989/scs.2014.16.4.339

Nonlinear cylindrical bending analysis of E-FGM plates with variable thickness

Abdelhakim Kaci [1], Khalil Belakhdar [*1],
Abdelouahed Tounsi [2] and El Abbes Adda Bedia [2]

[1] *Department of Civil Engineering and Hydraulics, University of Saida, Algeria*
[2] *Laboratory of Materials and Hydrology, University of Sidi Bel Abbes, Algeria*

(*Received November 05*, *2012*, *Revised November 04*, *2013*, *Accepted November 11*, *2013*)

Abstract. This paper presents a study of the nonlinear cylindrical bending of an exponential functionally graded plate (simply called E-FG) with variable thickness. The plate is subjected to uniform pressure loading and his geometric nonlinearity is introduced in the strain–displacement equations based on Von-Karman assumptions. The material properties of functionally graded plates, except the Poisson's ratio, are assumed to vary continuously through the thickness of the plate in accordance with the exponential law distribution; and the solution is obtained using Hamilton's principle for constant plate thickness. In order to analyze functionally graded plate with variable thickness, a numerical solution using finite difference method is used, where parabolic variation of the plate thickness is studied. The results for E-FG plates are given in dimensionless graphical forms; and the effects of material and geometric properties on displacements and normal stresses through the thickness are determined.

Keywords: functionally graded materials; nonlinear cylindrical bending; variable plate thickness; FGM

1. Introduction

Traditional composites which are usually composed of two different materials have been broadly used to fulfill the increasing high performance industrial demands. However, due to discontinuity of material properties at the interface of composite constituents, the stress fields in this region under some loading conditions such as high-temperature environment show some kind of singularity. For example, in the combustion chamber of air vehicle engines or a nuclear fusion reaction container, the relatively higher mismatch in thermal expansion coefficients of constituent materials will induce high residual stresses which may consequently lead to cracking or debonding. To eliminate the stress singularities in ultra-high-temperature environments, the concept of functionally graded materials (FGMs) was first introduced in 1984 by a group of material scientists in Japan (Niino and Maeda 1990, Hirano *et al.* 1988).

In FGMs, which are microscopically inhomogeneous and assumed to be a kind of composite material, the mechanical properties vary smoothly and continuously from one surface to the other. This is achieved by gradually varying the volume fraction of the constituent materials. By

∗Corresponding author, DR., E-mail: be.khalil@gmail.com

Copyright © 2014 Techno-Press, Ltd.
http://www.techno-press.org/?journal=scs&subpage=8 ISSN: 1229-9367 (Print), 1598-6233 (Online)

incorporating the variety of possibilities inherent with the FGM concept, new property functions are tailored and the materials performance in harsh environments could be improved. The FGM plates are widely being used in different thin-walled structures; and therefore, it is important to study and understand the nonlinear behaviour of functionally graded plates under pressure loadings.

Many different theories and solutions can be found in the literature, these methods differ to one another in terms of complexity and accuracy. For example studies like Tanigawa *et al.* (1996), Mizuguchi and Ohnabe (1996), Praveen *et al.* (1999), and Reddy *et al.* (1999) are based on linear thermal bending of FGM plates. Other studies investigated the non-linear analysis of FGM plates under thermal or mechanical loading like Praveen and Reddy (1998) where he investigated the response of functionally graded (FG) ceramic-metal plates using a plate finite element that accounts for the transverse shear strains, rotary inertia and moderately large rotations in the von Kármán sense. Reddy (2000) presented solutions for rectangular functionally graded plates based on the third-order shear deformation plate theory. The large deflection of FG plates under pressure load was studied using the von Karman strains by GhannadPour and Alinia (2006). Through-the-thickness stress distribution in the aluminum and alumina plates is linear whereas for the FG plates the behavior is nonlinear and is governed by the variation of the properties in the thickness direction. Using a similar method employed by Sun and Chin (1988, 1991), Navazi *et al.* (2006) performed nonlinear cylindrical bending analysis of FG plates based on the Classical Plate Theory (CPT). Additionally, a simple analytical solution based on classical plate theory was presented by Kaci *et al.* (2012) where they studied the nonlinear cylindrical bending of simply supported functionally graded nanocomposite plates reinforced by single-walled carbon nanotubes under uniform pressure loading in thermal environments in order to evaluate the effect of the material distribution on the deflections and stresses.

Other advanced solutions that take into account high-order plate theories (Zenkour 2007 and Matsunaga 2008) enhance the solution accuracy especially in thick plates. As an example Hiroyuki (2009) presented a two-dimensional higher-order deformation theory based on power series expansion for the evaluation of displacements and stresses in FG plates subjected to thermal and mechanical loadings. Bouderba *et al*. (2013) presented a thermomechanical bending analysis of FGM plates resting on Winkler-Pasternak elastic foundations. The solution is based on the refined trigonometric shear deformation theory (RTSDT) which yields only four unknowns to be solved without using shear correction factor. Moreover, other exact solution based on three-dimensional theory of elasticity are available in the literature such as Zhong and Shang (2003), Yepeng and Ding (2009), Kashtalyan (2004), and Yas (2011).

It should be mentioned that plates with constant thickness have being deeply studied. However, Athe variable thickness plates have also received the attention of designers and researches. Such modification in shape can improve the smoothness of the stress distribution and also can help in decreasing the geometrical discontinuities. However, studies on variable thickness plates using either closed form solution or numerical methods are limited in number. Fertis and Mijatov (1989) developed a general method to solve variable thickness plates based on equivalent flat plates. Xu and Zhou (2008) presented the three dimensionally elasticity solution for simply supported rectangular plates with variable thickness. Efraim and Eisenberger (2007) studied the vibration of variable thickness thick annular isotropic and FGM plates where the equations of motion including the effect of shear deformations using the first-order shear deformation theory are derived and exact solution for vibration frequencies and modes are obtained. Pradhan and Sarkar (2009) studied bending, buckling and vibration analysis of tapered beams made of functionally graded

materials using Eringen non-local elasticity theory and the associated governing differential equations are solved using Rayleigh-Ritz method. Other simple procedure is presented by Atmane *et al*. (2011) where he studied the free vibration of sigmoid functionally graded beams with variable cross-section based on Bernoulli-Euler beam theory.

It is intended here to accurately determine the displacements and stresses in exponential functionally graded plates in cylindrical bending subjected to uniform pressure. To this end, based on Classical Plate Theory (CPT) the governing equations are obtained. It should me mentioned that The CPT is a powerful and relatively accurate for thin plates. By using the von Karman nonlinear strains and gradual variation of material properties, the nonlinear equilibrium equations are obtained and then reduced to a linear differential equation. This equation is solved for simply supported BCs. After that a finite difference method is developed to have the ability of including the plate thickness variation. The effects of many parameters such material properties, loading, and plate shape and dimensions are studied.

2. Theoretical formulations

2.1 Properties of the E-FGM constituent materials

In this study, elastic rectangular E-FG plates having uniform thickness h and length $l = 2a$, are considered. Plates are made of a mixture of ceramics and metals; and it is assumed that their composition is gradual and that they are smoothly varied from the ceramic-rich top surface of the plate ($z = +h/2$) to the metal rich bottom surface ($z = -h/2$). As a consequence, the material properties of FGM plates, such as the Young's modulus E is function of depth z, measured from the middle plane of plate.

There are many analytical and computational models that discuss the issue of obtaining suitable functions for material properties of FGMs. Also, there are several criterions for selecting the most suitable function. These functions are meant to be simple and continuous, and should have the ability to exhibit curvatures, both ''concave upwards" and ''concave downwards" (Markworth *et al*. 1995). In the present study, an exponential law which does not present curvatures in both directions is utilized. The functional relationship between E and z for the ceramic–metal FGM plates is given in the below equation; as explained by Sallai *et al.* (2009)

$$E(z) = A\, e^{B(z+h/2)} \tag{1}$$

with

$$A = E_2 \quad \text{and} \quad B = \frac{1}{h}\ln\left(\frac{E_1}{E_2}\right) \tag{2}$$

where $E(z)$ indicates a typical Young's modulus and E_1 and E_2 denote Young's modulus of the bottom (i.e., $z = +h/2$) and top surface (i.e., $z = -h/2$), respectively.

2.2 *Governing equations for nonlinear cylindrical bending of E-FGM plates*

The fundamental equations of large deflection analysis of pressure loaded functionally graded plates are briefly outlined in this section. The classic plate theory (CPT) is applied throughout the work. As a result of the CPT assumptions, the Kirchhoff normalcy condition is incorporated,

therefore

$$u(x,y,z) = u_0(x,y) - z\frac{\partial w_0}{\partial x} \tag{3}$$

$$v(x,y,z) = 0 \tag{4}$$

$$w(x,y,z) = w_0(x,y) \tag{5}$$

where (u, v, w) are the displacements in the (x, y, z) directions, respectively. Also (u_0, v_0, w_0) are the displacements of the mid- plane in the (x, y, z) directions, respectively.

The nonlinear von Karman strain–displacement relations are used as follows

$$\varepsilon_x = \frac{\partial u_0}{\partial x} + \frac{1}{2}\left(\frac{\partial w_0}{\partial x}\right)^2 - z\frac{\partial^2 w_0}{\partial x^2} \tag{6}$$

$$\varepsilon_y = \varepsilon_z = 0 \tag{7}$$

$$\gamma_{xy} = \left(\frac{\partial u_0}{\partial y} + \frac{\partial v_0}{\partial x} + \frac{\partial w_0}{\partial x}\frac{\partial w_0}{\partial y}\right) - 2z\frac{\partial^2 w_0}{\partial x \partial y};\quad \gamma_{xz} = \gamma_{yz} = 0 \tag{8}$$

The constitutive relations for nonzero strains are given by

$$\begin{Bmatrix} \sigma_x \\ \sigma_x \\ \tau_{xy} \end{Bmatrix} = \begin{bmatrix} Q_{11} & Q_{12} & 0 \\ Q_{12} & Q_{22} & 0 \\ 0 & 0 & Q_{66} \end{bmatrix} \begin{Bmatrix} \varepsilon_x \\ \varepsilon_x \\ \gamma_{xy} \end{Bmatrix} \tag{9}$$

Using the material properties defined in Eq. (1), stiffness coefficients, Q_{ij}, can be expressed as

$$Q_{11} = Q_{22} = \frac{E(z)}{1-\nu^2} \tag{10}$$

$$Q_{12} = \frac{\nu\, E(z)}{1-\nu^2} \tag{11}$$

$$Q_{66} = \frac{E(z)}{2(1+\nu)} \tag{12}$$

Use of Hamilton's principle yields the Euler–Lagrange equations as (see Reddy 2003)

$$N_{x,x} = 0 \tag{13}$$

$$Q_{x,x} + q + N_x w_{,xx} = 0 \tag{14}$$

$$M_{x,x} - Q_x = 0 \tag{15}$$

Where q is the transverse load. The stress, shear force and moment resultants are defined as follows

$$\left(N_x, Q_x\right) = \int_{-h/2}^{h/2} \left(\sigma_x, \tau_{xy}\right) dz \quad \text{and} \quad M_x = \int_{-h/2}^{h/2} \sigma_x z \, dz \tag{16}$$

From Eqs. (13) one can conclude that

$$N_x = N_x^0 = const. \tag{17}$$

Consequently, Eqs. (14) and (15) become

$$M_{x,xx} + q + N_x^0 w_{,xx} = 0 \tag{18}$$

Upon substitution of Eqs. (6), (7), and (8) into Eqs. (9) and the subsequent results into Eq. (16), the generalized stress resultants in terms of displacement components will be obtained which can be presented as follows

$$N_x = A_{11}\left(u_{,x} + \frac{1}{2} w_{,x}^2\right) - B_{11} w_{,xx} \tag{19}$$

$$M_x = B_{11}\left(u_{,x} + \frac{1}{2} w_{,x}^2\right) - D_{11} w_{,xx} \tag{20}$$

A_{11}, B_{11} and D_{11} are called extension, bending-extension coupling, and bending stiffness coefficients, respectively, and are defined as follows

$$\left(A_{11}, B_{11}, D_{11}\right) = \int_{-h/2}^{h/2} Q_{11}\left(1, z, z^2\right) dz \tag{21}$$

Substituting Eq. (20) into Eq. (21) yields

$$M_x = \frac{B_{11}}{A_{11}} N_x^0 + \left(\frac{B_{11}^2}{A_{11}} - D_{11}\right) w_{,xx} \tag{22}$$

By substituting Eq. (22) into Eq. (18), one can obtain

$$w_{,xxxx} - k^2 w_{,xx} = q_0 \tag{23}$$

where

$$k^2 = \frac{N_x^0}{\left(D_{11} - \dfrac{B_{11}^2}{A_{11}}\right)} \tag{24}$$

$$q_0 = \frac{q}{\left(D_{11} - \dfrac{B_{11}^2}{A_{11}}\right)} \tag{25}$$

3. Analytical solution

In this study it is assumed that an E-FG plate is subjected to a uniform transverse load q on its top surface. It is intended here to obtain analytical solution for the non-linear bending of the E-FG plate.

Eq. (23) is a linear fourth-order ordinary differential equation whose solution is readily available. The general solution is as follows

$$w(x) = C_1 \cosh(kx) + C_2 - \frac{q_0}{2k^2} x^2 \tag{26}$$

where C_1 and C_2 are constants, which must be determined using BCs at either edges of the plate. Assume that the origin of the coordinate system is located at the plate mid-span; accordingly, the simply supported BCs yield

$$w(a) = w(-a) = 0 \tag{27}$$

$$M_x(a) = M_x(-a) = 0 \tag{28}$$

$$u(a) = u(-a) = 0 \tag{29}$$

Since N_x is an unknown constant along the x-axis, the in-plane displacement u can be derived by integrating Eq. (13) over the span of the plate, using the general solution shown in Eq. (26). The boundary conditions can be expressed as

$$w(a) = 0 \tag{30}$$

$$M_x(a) = \frac{B_{11}}{A_{11}} N_x^0 - \left(D_{11} - \frac{B_{11}^2}{A_{11}} \right) w_{,xx} \Big|_{x=a} = 0 \tag{31}$$

$$u(a) = \int_0^a \left(\frac{N_x^0}{A_{11}} + \frac{B_{11}}{A_{11}} w_{,xx} - \frac{1}{2} w_{,x}^2 \right) dx = 0 \tag{32}$$

Substitution of Eq. (26) into Eqs. (30)-(32) and evaluating the integral in Eq. (32) yield

$$C_1 = \left(\frac{B_{11}}{A_{11}} + \frac{q_0}{k^4} \right) \frac{1}{\cosh(ka)} \tag{33}$$

$$C_2 = \frac{q_0 a^2}{2k^2} - C_1 \cosh(ka) \tag{34}$$

$$\begin{aligned} u(a) = {} & \frac{N_x^0}{A_{11}} a + \frac{B_{11}}{A_{11}} k C_1 \sinh(ka) - \frac{B_{11}}{A_{11}} \frac{q_0}{k^2} a - \frac{1}{2} k^2 C_1^2 \left(\frac{1}{4k} \sinh(2ka) - \frac{a}{2} \right) \\ & - \frac{q_0^2 a^3}{6k^4} + C_1 \frac{q_0}{k^3} \left[ka \cosh(ka) - \sinh(ka) \right] = 0 \end{aligned} \tag{35}$$

These three equations contain three unknown quantities: C_1, C_2 and N_x^0; and a numerical technique must be used to obtain the solution.

4. Finite difference solution

The differential equation, Eq. (23), is valid for FGM plate with constant thickness along its length. However, in case of variable thickness plate the closed form solution is complex. Thus, in such case the finite difference method can be used effectively to evaluate the behavior of FGM plates with variable thickness.

A finite difference solution using constant node spacing, Δh, is outlined below. The finite difference mesh contains $n + 4$ nodes, where the nodes are numbered with real nodes from $x = a$ to $x = -a$, in addition to virtual nodes (1, 2, $n + 3$, $n + 4$) which are used to allow derivatives to be defined at nodes 3 and $n + 2$. Subscripts are used to define nodes' numbers in the equations.

In finite difference format, Eq. (23) can be written as follows

$$\frac{1}{\Delta h^4}\left(w_{(i-2)} - 4w_{(i-1)} + 6w_{(i)} - 4w_{(i+1)} + w_{(i+2)}\right) - \frac{k_{(i)}^2}{\Delta h^2}\left(w_{(i-1)} - 2w_{(i)} + w_{(i+1)}\right) = q_{0(i)} \tag{36}$$

where

$$k_{(i)}^2 = \frac{N_{x\,(i)}^0}{\left(D_{11_{(i)}} - \dfrac{B_{11_{(i)}}^2}{A_{11_{(i)}}}\right)} \tag{37}$$

$$q_{0_{(i)}} = \frac{q_{(i)}}{\left(D_{11_{(i)}} - \dfrac{B_{11_{(i)}}^2}{A_{11_{(i)}}}\right)} \tag{38}$$

It should be noted that $N_{x(i)}^0$ and $q_{(i)}$ are considered to be constant along the plate.

So, the equation can be simplified as

$$w_{(i-2)} + \left(-4 - k_{(i)}^2\Delta h^2\right)w_{(i-1)} + \left(6 + 2k_{(i)}^2\Delta h^2\right)w_{(i)} + \left(-4 - k_{(i)}^2\Delta h^2\right)w_{(i+1)} + w_{(i+2)} = q_{0(i)}\Delta h^4;\ \ i = 4\ldots(n+1) \tag{39}$$

Noting that when applying this equation at node 4 and node $(n + 1)$ we will have two virtual nodes which are node 2 and node $(n + 3)$.

Application of boundary equations

- The deflection $w(-a) = 0$ so, at node 3 we have $w_{(3)} = 0$
- The deflection $w(a) = 0$ so, at node $(n + 2)$ we have $w_{(n+2)} = 0$
- The moment $M_x(-a) = 0$, and since $w_{(3)} = 0$, the Eq. (30) can be written after simplification as follows

$$\left(w_{(2)} + w_{(4)}\right) = -\frac{B_{11_{(3)}} N_x^0 \Delta h^2}{A_{11_{(i)}}\left(\dfrac{B_{11_{(3)}}^2}{B_{11_{(3)}}^2} - D_{11_{(3)}}\right)} \tag{40}$$

This equation is then used to eliminate the virtual node 2 by substituting it in the global Eq. (23) at node 4 where we get

$$\left(5+2k_{(4)}^2\Delta h^2\right)w_{(4)}+\left(-4-k_{(4)}^2\Delta h^2\right)w_5+w_{(6)}=q_{0(4)}\Delta h^4+\frac{B_{11_{(3)}}N_x^0\Delta h^2}{A_{11_{(3)}}\left(\dfrac{B_{11_{(3)}}^2}{A_{11_{(3)}}}-D_{11_{(3)}}\right)} \tag{41}$$

- The moment $M_x(a) = 0$, and considering that $w_{(n+2)} = 0$, the Eq. (31) can be written after simplification as follows

$$\left(w_{(n+1)}+w_{(n+3)}\right)=-\frac{B_{11_{(n+2)}}N_x^0\Delta h^2}{A_{11_{(n+2)}}\left(\dfrac{B_{11_{(n+2)}}^2}{A_{11_{(n+2)}}}-D_{11_{(n+2)}}\right)} \tag{42}$$

This equation is then used to eliminate the virtual node $(n + 3)$ by substituting it in the global Eq. (39) at node $(n + 1)$ where we get

$$w_{(n-1)}+\left(-4-k_{(n+1)}^2\Delta h^2\right)w_n+\left(5+2k_{(n+1)}^2\Delta h^2\right)w_{(n+1)}=q_{0(n+1)}\Delta h^4+\frac{B_{11_{(n+2)}}N_x^0\Delta h^2}{A_{11_{(n+2)}}\left(\dfrac{B_{11_{(n+2)}}^2}{A_{11_{(n+2)}}}-D_{11_{(n+2)}}\right)} \tag{43}$$

Finally, the combination of Eqs. (39), (41), (43) yields the following system of equations

$$\begin{bmatrix}
1 & & & & & & & & \\
0 & \left(5+2k_{(4)}^2\Delta h^2\right) & \left(-4-k_{(4)}^2\Delta h^2\right) & 1 & & & & & \\
1 & \left(-4-k_{(5)}^2\Delta h^2\right) & \left(6+2k_{(5)}^2\Delta h^2\right) & \left(-4-k_{(5)}^2\Delta h^2\right) & 1 & & & & \\
 & & & & \ddots & & & & \\
 & & & & 1 & \left(-4-k_{(n)}^2\Delta h^2\right) & \left(6+2k_{(n)}^2\Delta h^2\right) & \left(-4-k_{(n)}^2\Delta h^2\right) & 1 \\
 & & & & & 1 & \left(-4-k_{(n+1)}^2\Delta h^2\right) & \left(5+2k_{(n+1)}^2\Delta h^2\right) & 0 \\
 & & & & & & & & 1
\end{bmatrix}
\begin{Bmatrix} w_{(3)} \\ w_{(4)} \\ w_{(5)} \\ \vdots \\ w_{(n)} \\ w_{(n+1)} \\ w_{(n+2)} \end{Bmatrix}$$

$$=\begin{Bmatrix}
0 \\
q_{0(4)}\Delta h^4+\dfrac{B_{11_{(3)}}N_x^0\Delta h^2}{A_{11_{(3)}}\left(\dfrac{B_{11_{(3)}}^2}{A_{11_{(3)}}}-D_{11_{(3)}}\right)} \\
q_{0(5)}\Delta h^4 \\
\vdots \\
q_{0(n)}\Delta h^4 \\
q_{0(n+1)}\Delta h^4+\dfrac{B_{11_{(n+2)}}N_x^0\Delta h^2}{A_{11_{(n+2)}}\left(\dfrac{B_{11_{(n+2)}}^2}{A_{11_{(n+2)}}}-D_{11_{(n+2)}}\right)} \\
0
\end{Bmatrix} \tag{44}$$

The above n simultaneous equations cannot be solved since the constant N_x^0 is not known. On the other hand, the boundary equation presented by Eq. (32) must be satisfied. Therefore, the idea is to find the correct value of N_x^0 that makes $u(a) = 0$.

Since N_x^0 is constant along the plate (x-direction), the trial and error technic is used to evaluate N_x^0, where at the first iteration an initial value equals to zero is assigned to N_x^0, then the simultaneous equations are solved. After that and according to Eq. (32), the axial displacement $u(x)$ is evaluated using finite difference method as follows

$$u(i)=\frac{N_{x(i)}^0}{A_{11_{(i)}}}+\frac{B_{11_{(i)}}}{A_{11(i)}}\frac{1}{\Delta h^2}\left(w_{(i-1)}-2w_{(i)}+w_{(i+1)}\right)-\frac{1}{2}\left(\frac{1}{2\Delta h}\left(-w_{(i-1)}+w_{(i+1)}\right)\right)^2 \tag{45}$$

Numerical integration technic using trapezoidal method is then used to evaluate $u(a)$

$$u(a)=\frac{\Delta h}{2}\sum_{n_0}^{n+1}\left(u(i)+u(i+1)\right) \tag{46}$$

Where n_0 is the middle node that corresponds to $x = 0$, $n_0=\dfrac{(n+4)+1}{2}$.

The obtained value of $u(a)$ (at the first iterations its value almost dose not equal to zero), is used to estimate a new value of N_x^0 using a simple linear interpolation.

In the second iteration, the new value of N_x^0 is used to solve the simultaneous equations (Eq. (44)). The same above steps are followed until the value of N_x^0 converges to a value that satisfies the following tolerance ε

$$\varepsilon \geq \frac{\left\|\left(N_x^0\right)_{step:(i+1)}-\left(N_x^0\right)_{step:(i)}\right\|}{\left(N_x^0\right)_{step:(i)}} \tag{47}$$

It is noted that the value of N_x^0 converges very fast since it depends linearly to the value of $u(a)$ where, when using a tolerance of $\varepsilon = 0.0001$, the solution converges mostly after 5 to 10 iterations.

5. Numerical results and discussion

It is assumed that the Young's modulus at the top surface of the E-FGM plate, E_2, is 70 GPa, while that at the bottom surface of the E-FGM plate, E_1, varies with the ratio of E_1/E_2. Note that Poisson's ratio is selected constant and equal to 0.3 for both of the constituents. The plate geometry is chosen so the $h = 5$ mm and $a = 0.5$ m. The results obtained from the analysis are presented in dimensionless parametric terms of displacements and stresses as follows

- side coordinate $\bar{x} = x / a$,
- thickness coordinate $\bar{z} = z / h$,
- transvers deflection $\bar{w} = w / h$,
- axial displacement $\bar{u} = u / a$,
- axial stress $\bar{\sigma}_x = \sigma_x / [Q_{11m}(h / a)^2]$, ($Q_{11m}$ stiffness coefficient of metal plate),
- load parameter $q^n = q_0 a^4 / (E_m h^4)$.

5.1 Analytical solution Vs. finite difference solution

The adopted mesh density (number of nodes) was chosen according to Fig. 1 which presents

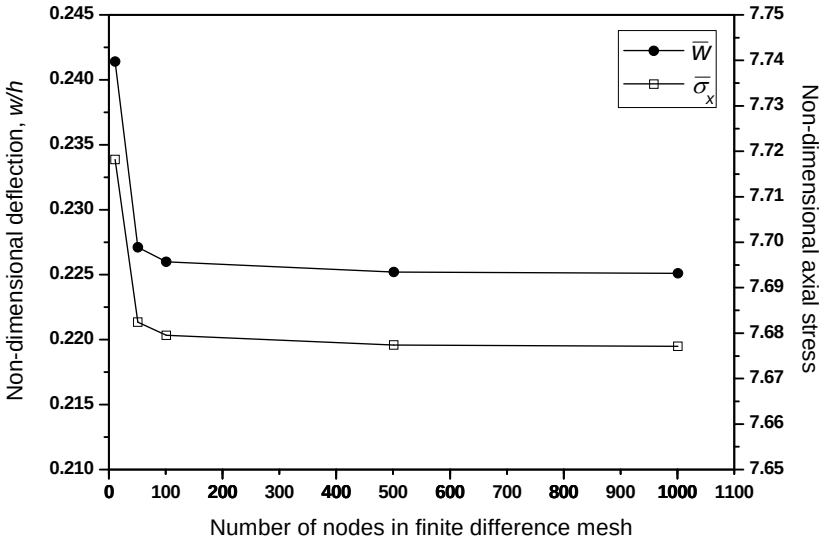

Fig. 1 convergence of finite difference solution

the solution convergence in terms of the mesh density where it is clear that the solution converges fast and using mesh with 1001 nodes is sufficient in terms of accuracy. Thus, the number of nodes used in the finite difference (FD) mesh was 1001 nodes, and this value was kept for all the FD analysis.

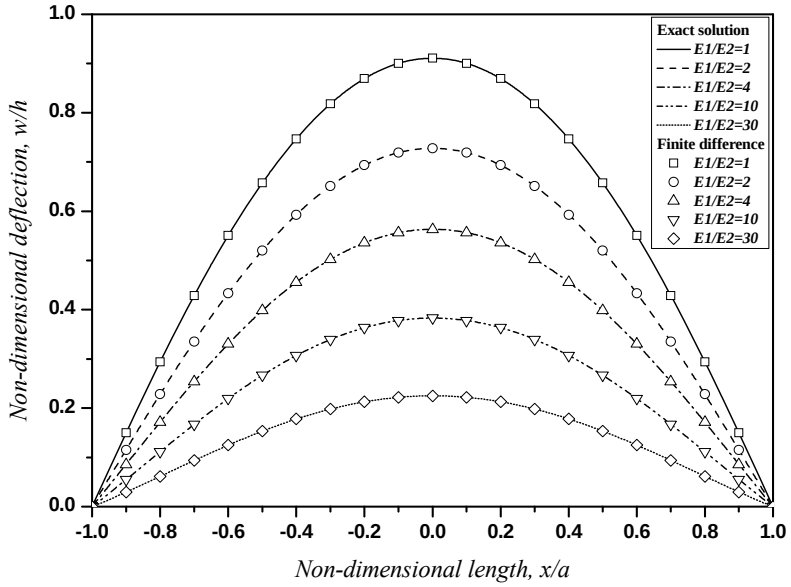

Fig. 2 Non-dimensional deflections due to transverse load q = 1 kN/m^2 versus non-dimensional length for different E_1/E_2

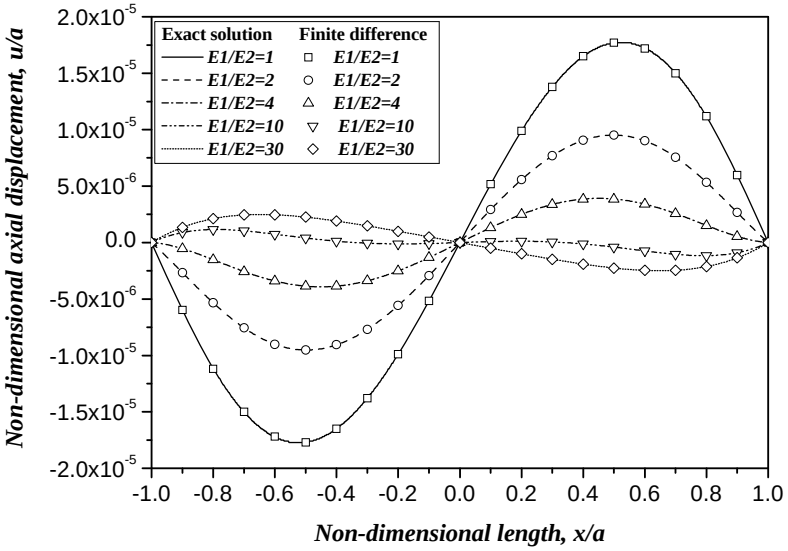

Fig. 3 Non-dimensional axial displacement due to transverse load q = 1 kN/m^2 versus non-dimensional length for different E_1/E_2

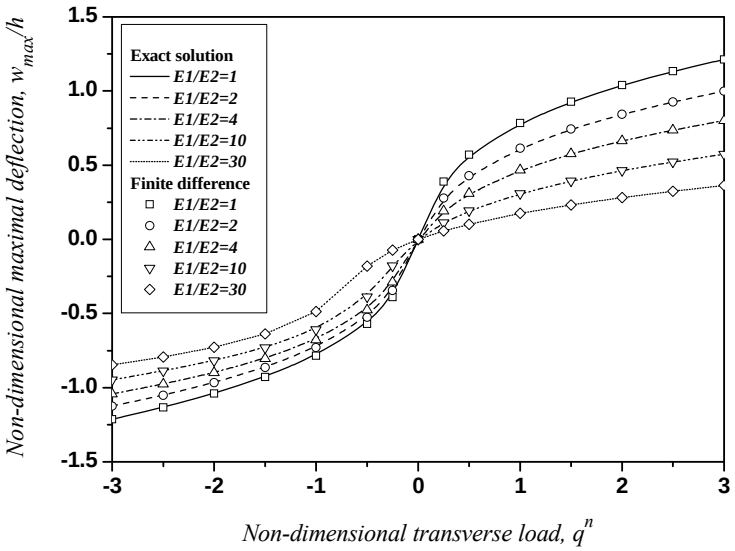

Fig. 4 Variation of the non-dimensional center deflection $\bar{w}_{\max}$ of the E-FG plate versus q^n for different E_1/E_2

In point of view of comparison between the exact solution and finite difference solution for constant plate thickness, all Figs. 2-5 show perfect agreement between the two solutions.

5.2 Effect of E_1/E_2 on E-FG plate with constant thickness

Figs. 2 and 3 illustrate the variation of the non-dimensional deflection and axial displacement

versus non-dimensional length for different ration of E_1/E_2, respectively. The curves shows the more E_1/E_2 ratio, the smaller displacements (for $\bar{w}$ and $\bar{u}$), because of the great stiffness of the E-FG plate for larger E_1/E_2.

Fig. 4 illustrates the variation of the non-dimensional center deflection of the E-FG plate with different E_1/E_2 subjected to a uniform transverse load. The results show that the homogeneous plate ($E_1/E_2 = 1$) has highest deflection. Besides, the plate exhibits different behaviors in positive and negative transverse loadings. In negative loading, at the beginning of loading, the analysis yields larger deflections. However, in positive loading, we remark an important effect of E_1/E_2 than the case of negative loading.

Fig. 5 show through the thickness distributions of the non-dimensional axial stress $\bar{\sigma}_x$ of the E-FG plate subjected to q = 1 kN/m^2 for different E_1/E_2. Under the application of the pressure loading, the stresses are compressive at the bottom surface and tensile at the top surface. From this figure it can be observed that as the ratio of E_1/E_2 increases, the magnitudes of the tensile stresses increase while the compression stresses at the bottom surface do not affected significantly.

5.3 Effect of E_1/E_2 on E-FG plate with variable thickness

Herein the effect of E-FG plate with variable thickness is presented. The thickness of the E-FG plate is described by arbitrary function of the longitudinal coordinate x; $h = h(x)$. Two parabolic variation has been adopted, parabolic concave and parabolic convex, where the thickness has the variation indicated by Eq. (48) (see Fig. 6) .The thickness at the end is kept constant (5 mm), while two values are assigned to the thickness of the plate at the dim-span, 2.5 mm and 7.5 mm.

$$h(x) = \frac{\left(h_e - h_c\right)}{a^2} x^2 + h_c \tag{48}$$

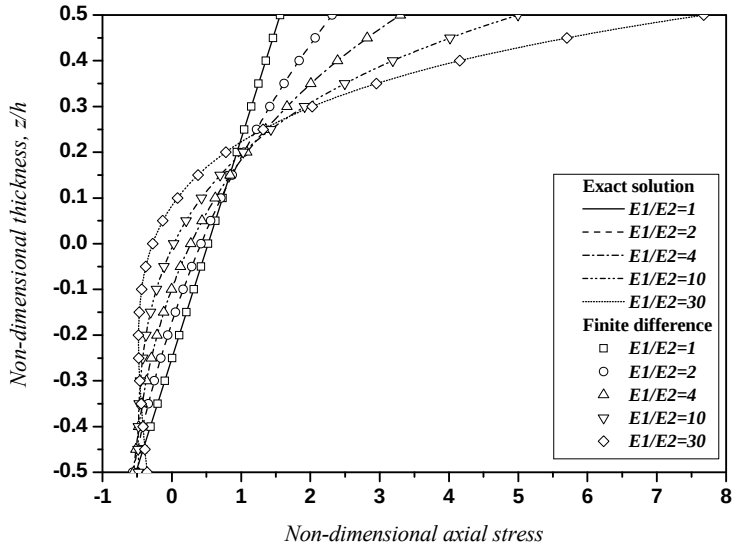

Fig. 5 Through the thickness distribution of non-dimensional axial stress $\bar{\sigma}_x$ of the E-FG plate subjected to q = 1 kN/m^2 for different E_1/E_2

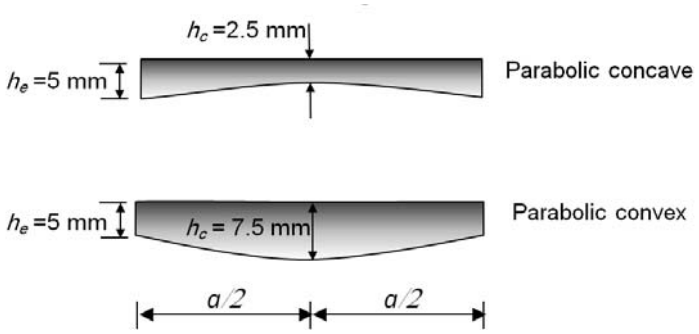

Fig. 6 E-FG plate parabolic thickness variation

Where he is the plate end-thickness (at $x = \pm a$), and h_c is the thickness at mid-span (at $x = 0$).

Fig. 7 presents the variation of the maximum deflection $w_{\max}$ versus the ratio E_1/E_2 for different E-FG mid-span thicknesses. According to Fig. 7, it can be noted the mid-span thickness has a significant effect on the maximum deflection, where, as the mid-span thickness increases, the maximum deflection decreases. Besides, the effect of the ratio E_1/E_2 on the maximum deflection is almost the same form for different plate mid-span thicknesses.

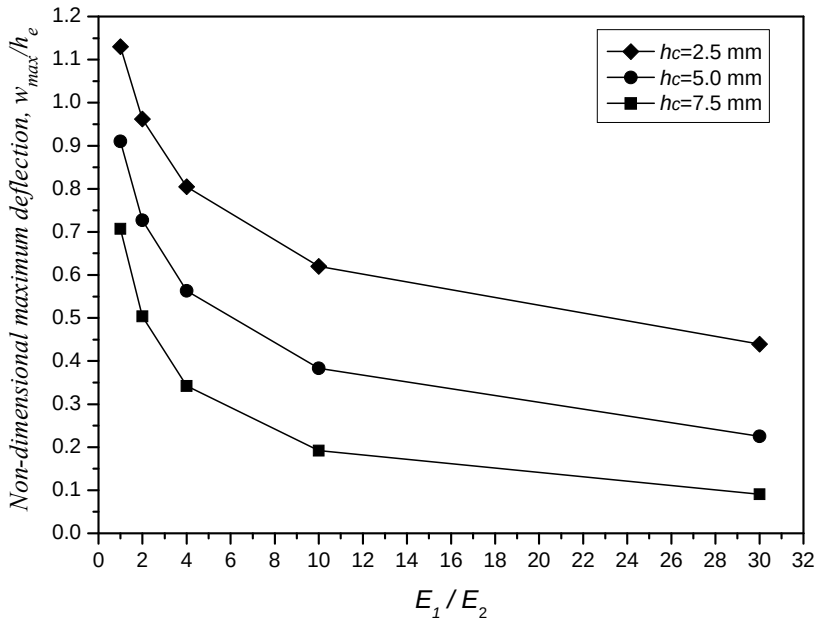

Fig. 7 Effect of E_1/E_2 and E-FG mid-span thickness (h_c) on the non-dimensional maximum deflection due to transvers load q = 1 kN/m^2

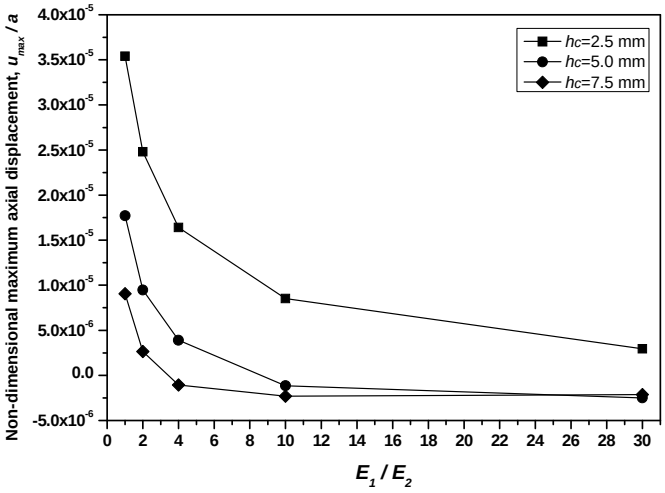

Fig. 8 Effect of E_1/E_2 and E-FG mid-span thickness on the non-dimensional maximum axial displacement due to transvers load q = 1 kN/m^2

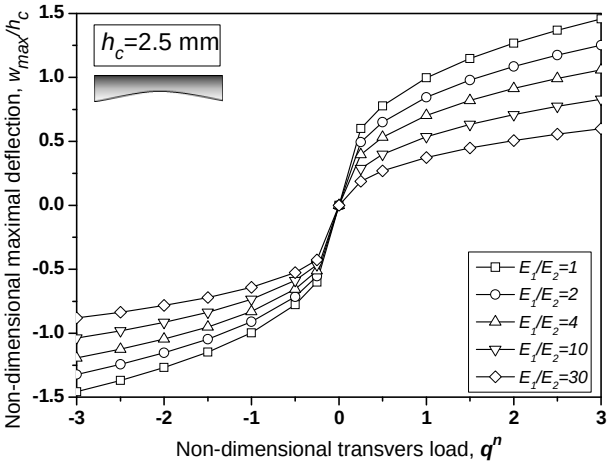

Fig. 9 Variation of the non-dimensional deflection $\bar{w}_{\max}$ of the E-FG plate versus q^n and E_1/E_2 for E-FG plate with mid-span thickness h_c = 2.5 mm

Fig. 8 shows the effect of the ratio of E_1/E_2 on the axial displacement for E-FG plate with different mid-span thicknesses. It can be noted that as the mid-span thickness increases, the axial maximum displacement decreases. However, increasing mid-span thickness of E-FG has a negligible effect on the maximum axial displacement for values of E_1/E_2 greater than 10.

Figs. 9 and 10 present the effect of transvers load on the maximum deflection for different E_1/E_2 ration and E-FG mid-span thicknesses. Again, the curves reveal that the smaller the E-FG mid-span thickness is, the greater the deflection is. Besides, for E_1/E_2 = 30, the effect of load variation on the deflection becomes insignificant when the mid-span thickness of the E-FG plate is

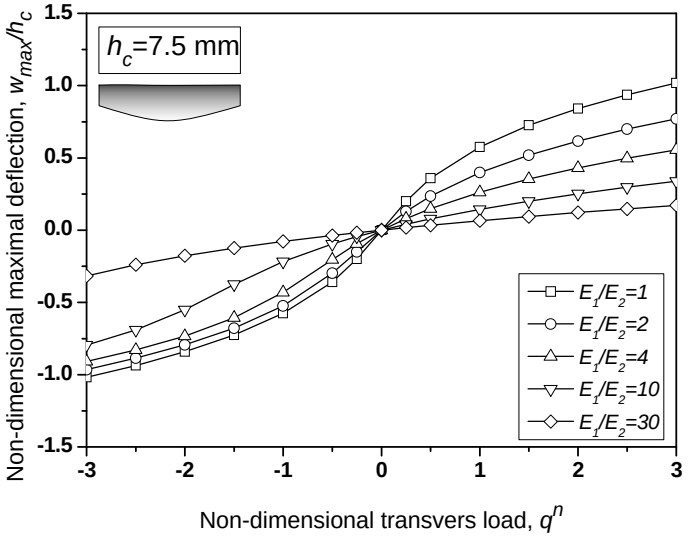

Fig. 10 Variation of the non-dimensional deflection $\bar{w}_{\max}$ of the E-FG plate versus q^n and E_1/E_2 for E-FG plate with mid-span thickness h_c = 7.5 mm

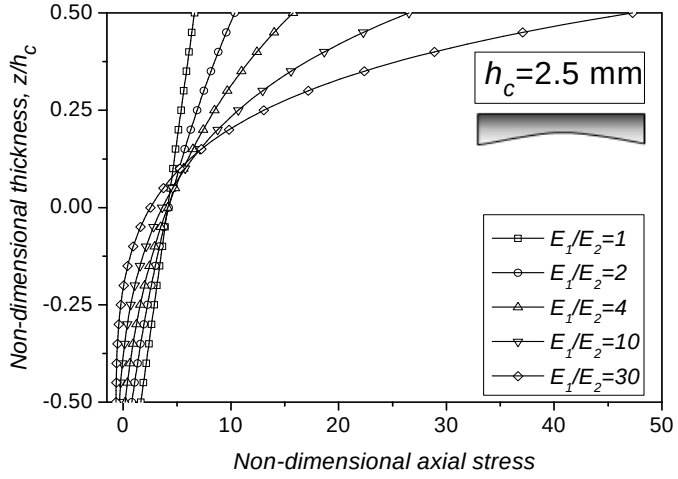

Fig. 11 Through the thickness distribution of non-dimensional axial stress $\bar{\sigma}_x$ of the E-FG plate having mid-span thickness of h_c = 2.5 mm for different E_1/E_2

greater than its ends. In addition, the maximum deflection versus transvers load curve becomes smoother for grater E_1/E_2 and thicker E-FG mid-span thickness.

Therefore, according to the above curves of displacements (transvers and normal displacements), the displacements (transvers and axial displacements) are noticed to be highly dependent on the E-FG stiffness. The latter is related to the material properties; that's to say the ratio E_1/E_2 and the geometric properties i.e., m E-FG mid-span thickness. Thus the greater the stiffness is (higher E_1/E_2 and/or thicker mid-span), the lower the displacements are and vice versa.

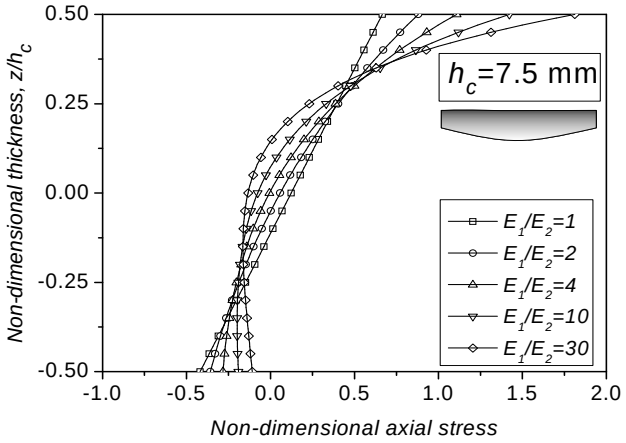

Fig. 12 Through the thickness distribution of non-dimensional axial stress $\bar{\sigma}_x$ of the E-FG plate having mid-span thickness of h_c = 7.5 mm for different E_1/E_2

The effect of E_1/E_2 ration and E-FG mid-span thickness on the axial stress is shown in Figs. 11-12). The results show that the E-FG mid-span thickness significantly affect the axial stress, where, when increasing the plate mid-span thickness by 50% (from 5 mm to 7.5 mm) leads in decreasing the axial stresses to the quarter (from 7.68 to 1.81). While, decreasing the plate mid-span thickness by 50% (from 5 mm to 2.5 mm) leads to a significant increase in the axial stresses up to 6 times (from 7.68 to 47.27).

6. Conclusions

The nonlinear cylindrical bending of the E-FG plates under pressure loading was studied. Fundamental equations for thin E-FG plates have been obtained using the Von-Karman tensor for large deflections. The material properties of E-FG plates were assumed to vary continuously through the thickness of plates; and were graded according to two power-law distributions. For the cylindrical bending problem, it is found that the plate Navier equations according to the large deflection theory can be expressed as linear equations for the deflection, leaving nonlinear boundary conditions. This linearity of the differential equations greatly simplifies the large deflection analysis. E-FG plates with variable thickness were also studied using finite difference method. Two types of parabolic thickness variations were adopted, parabolic concave and parabolic convex shapes with mid-span thickness equals to 50% and 150% of the end-plate thickness, respectively. The comparison between the exact solution and the finite difference solution of the differential equations shows that they are identical.

As a general conclusion, it was found that the thickness variation has a significant effect on the behaviour and stress distribution of the FGM. The results show that varying the E-FG plate thickness at its mid-span can affect the mid-span deflection and the axial displacement. In general, the displacements (trasvers and axial displacements) found to be greatly affected by the E-FG stiffness which is related to material properties (E_1/E_2) and geometric properties (E-FG mid-span thickness). Thus, the greater the stiffness is (higher E_1/E_2 and/or thicker mid-sapn), the lower the

displacements are and vice-versa.

On the other hand, the axial stresses were found to be significantly affected by the mid-span thickness variation especially for higher ratios of E_1/E_2, where for high ratio of E_1/E_2, a high axial stress can be obtained when reducing the E-FG mid-span thickness.

References

Atmane, H., Tounsi, A., Ziane, N. and Mechab, I. (2011), "Mathematical solution for free vibration of sigmoidfunctionally graded beams with varying cross-section", *Steel Comp. Struct., Int. J.*, **11**(6), 489-504.

Bouderba, B., Houari, M.S.A. and Tounsi, A. (2013), "Thermomechanical bending response of FGM thick plates resting on Winkler-Pasternak elastic foundations", *Steel Comp. Struct., Int. J.*, **14**(1), 85-104.

Efraim, E. and Eisenberger, M. (2007), "Exact vibration analysis of variable thickness thick annular isotropic and FGM plates", *J. Sound Vib.*, **299**(4-5), 720-738.

Fertis, D.G. and Mijatov, M.M. (1989), "Equivalent systems for variable thickness plates", *ASCE J. Eng. Mech.*, **115**(10), 2287-300.

GhannadPour, S.A.M. and Alinia, M.M. (2006), "Large deflection behavior of functionally graded plates under pressure loads", *Compos. Struct.*, **75**(1-4), 67-71.

Hirano, T., Yamada, T., Teraki, J., Niino, M. and Kumakawa, A. (1988), "A study on functionally gradient material design system for a thrust chamber", *Proceedings of the* 16*th International Symposium on Space Technology and Science*, Sapporo, Japan, May.

Hiroyuki, M. (2009), "Stress analysis of functionally graded plates subjected to thermal and mechanical loadings", *Compos. Struct.*, **87**(4), 344-357.

Kaci, A., Tounsi, A., Bakhti, K. and Bedia, E.A. (2012), "Nonlinear cylindrical bending of functionally graded carbon nanotube-reinforced composite plates", *Steel Comp. Struct., Int. J.*, **12**(6), 491-504.

Kashtalyan, M. (2004), "Three-dimensional elasticity solution for bending of functionally graded rectangular plates", *Europ. J. Mech. A/Solids*, **23**(5), 853-864.

Markworth, A.J., Ramesh, K.S. and Parks, W.P. (1995), "Modeling studies applied to functionally graded materials", *J. Mater. Sci.*, **30**(9), 2183-2193.

Matsunaga, H. (2008), "Free vibration and stability of functionally graded plates according to a 2-D higher-order deformation theory", *Compos. Struct.*, **82**(4), 499-512.

Mizuguchi, F. and Ohnabe, H. (1996), "Large deflections of heated functionally graded simply supported rectangular plates with varying rigidity in thickness direction", *Proceedings of the* 11*th Technical Conference of the American Society for Composites*, USA, pp. 957-966.

Navazi, H.M., Haddadpour, H. and Rasekh, M. (2006), "An analytical solution for nonlinear cylindrical bending of functionally graded plates", *Thin Wall. Struct.*, **44**(11), 1129-1137.

Niino, M. and Maeda, S. (1990), "Recent development status of functionally gradient materials", *ISIJ Int.*, **30**(9), 699-703.

Pradhan, S.C. and Sarkar, A. (2009), "Analyses of tapered FGM beams with nonlocal theory", *Struct. Eng. Mech., Int. J.*, **32**(6), 811-833.

Praveen, G.N., Chin, C.D. and Reddy, J.N. (1999), "Thermoelastic analysis of functionally graded ceramic–metal cylinder", *J. Eng. Mech. ASCE*, **125**(11), 1259-1267.

Praveen, G.N. and Reddy, J.N. (1998), "Nonlinear transient thermoelastic analysis of functionally graded ceramic-metal plates", *Int. J. Solids Struct.*, **35**(33), 4457-4476.

Reddy, J.N. (2000), "Analysis of functionally graded plates", *Int. J. Numer. Meth. Eng.*, **47**(1-3), 663-684.

Reddy, J.N., Wang, C.M. and Kitipornchai, S. (1999), "Axisymmetric bending of functionally grade circular and annular plates" *Euro. J. Mech. A/Solids*, **18**(2), 185-199.

Reddy, J.N. (2003), *Mechanics of Laminated Composite Plates and Shells, Theory and Analysis*, (2nd Ed.), CRC Press, Boca Raton, FL, USA.

Sallai, B.O., Tounsi, A., Mechab, I., Bachir Bouiadjra M., Meradjah, M. and Adda Bedia, E.A. (2009), "A theoretical analysis of flexional bending of Al/Al2O3 S-FGM thick beams", *Comp. Mater. Sci.*, **44**(4), 1344-1350.

Sun, C.T. and Chin, H. (1988), "Analysis of asymmetric composite laminates", *AIAA J.*, **26**(6), 714-718.

Sun, C.T. and Chin, H. (1991), "Cylindrical bending of unsymmetric composite laminates", *AIAA J.*, **30**(5), 1438-1440.

Tanigawa, Y., Akai, T., Kawamura, R. and Oka, N. (1996), "Transient heat conduction and thermal stress problems of a nonhomogeneous plate with temperature dependent material properties", *J. Therm. Stresses*, **19**(1), 77-102.

Xu, Y.P. and Zhou, D. (2008), "Three-dimensional elasticity solution for simply supported rectangular plates with variable thickness", *J. Strain Anal. Eng. Des.*, **43**(3), 165-176.

Yas, B., Aragh, S. and Heshmati, M. (2011), "Three-dimensional free vibration analysis of functionally graded fiber reinforced cylindrical panels using differential quadrature method", *Struct. Eng. Mech., Int. J.*, **37**(5), 529-542.

Yepeng, X. and Ding, Z. (2009), "Three-dimensional elasticity solution of functionally graded rectangular plates with variable thickness", *Compos. Struct.*, **91**(1), 56-65.

Zenkour, A.M. (2007), "Benchmark trigonometric and 3-D elasticity solutions for an exponentially graded thick rectangular plate", *Arch. Appl. Mech.*, **77**(4), 197-214.

Zhong, Z. and Shang, E.T. (2003), "Three-dimensional exact analysis of a simply supported functionally gradient piezoelectric plate", *Int. J. Solids Struct.*, **40**(20), 5335-5352.

CC